

# $^8\text{Li}$ electron spectrum versus $^8\text{B}$ neutrino spectrum: implications for the Sudbury Neutrino Observatory

G. Jonkmans<sup>1,2\*</sup>, I.S. Towner<sup>1</sup> and B. Sur<sup>2</sup>

<sup>1</sup> *Department of Physics, Queen's University, Kingston, Ontario, Canada K7L 3N6*

<sup>2</sup> *AECL, Chalk River Laboratories, Chalk River, Ontario, Canada K0J 1J0*

(November 17, 2018)

## Abstract

The sensitivity of the Sudbury Neutrino Observatory (SNO) to measure the shape of the recoil electron spectrum in the charged-current reaction of  $^8\text{B}$  solar neutrinos interacting with deuterium can be improved if the results of a  $^8\text{Li}$  beta-decay calibration experiment are included in the test. We calculate an improvement in sensitivity, under certain idealistic assumptions, of about a factor of 2, sufficient to resolve different neutrino-oscillation solutions to the solar-neutrino problem. We further examine the role of recoil and radiative corrections on both the  $^8\text{B}$  neutrino spectrum and the  $^8\text{Li}$  electron spectrum and conclude that the influence of these effects on the ratio of the two spectra as measured by SNO is very small.

13.15.-f, 23.40.Bw, 25.30.Pt, 96.60.Kx

Typeset using REVTeX

---

\*Present address: Institut de Physique, Université de Neuchâtel, CH-2000 Neuchâtel, Switzerland

## I. INTRODUCTION

The Sudbury Neutrino Observatory (SNO) [1] will utilize the interaction of  $^8\text{B}$  solar neutrinos with deuterium in heavy water to measure the shape of the recoil electron spectrum in charged-current (CC) interactions and the ratio of the number of charged-current to neutral-current (NC) events. In what follows, we will concentrate only on the test of the CC spectral shape, where one of the measurable quantities is the average kinetic energy of the detected recoil electrons,  $\langle T_e \rangle_\nu$ , to be defined more precisely below. The main uncertainties, other than counting statistics, arise from uncertainties in (a) the theoretical standard  $^8\text{B}$  neutrino spectrum, (b) the detector energy resolution and (c) the detector absolute energy scale. If the uncertainties from these sources can be reduced sufficiently SNO should be able to distinguish between a Standard Solar Model with no neutrino oscillations and one with various choices of neutrino oscillation scenarios [2]: a Small Mixing Angle (SMA), a Large Mixing Angle (LMA) or Vacuum Oscillations (VAC) solutions. One way to reduce these uncertainties is to introduce a  $^8\text{Li}$  calibration source. As part of its overall calibration strategy, the SNO collaboration will install a system that is capable of producing a  $^8\text{Li}$  source placed at several different locations inside the detector [3]. Detection of electrons from this source would demonstrate that the results obtained by SNO for a known beta-decay spectrum are consistent with those measured in the laboratory.

In this paper we point out that uncertainties in the measured CC spectral shape can be reduced considerably by a direct comparison with the measured beta-decay spectrum of  $^8\text{Li}$ . For instance, rather than considering  $\langle T_e \rangle_\nu$  to be the benchmark for comparing experiment with different theoretical expectations, we consider the ratio  $\langle T_e \rangle_\nu / \langle T_e \rangle_e$ , where  $\langle T_e \rangle_e$  is the average kinetic energy of detected electrons from  $^8\text{Li}$  decay. In forming ratios such as this, many uncertainties cancel producing a much improved error budget. This suggested analysis strategy is based upon the fact that the electron spectra from  $^8\text{Li}$  beta decay and from  $^8\text{B}$  solar-neutrino absorption on deuterium originate from mirror weak decays to common final states in  $^8\text{Be}^*$ , hence are highly correlated, have somewhat similar shapes and cover essentially the same energy range. In formulating this strategy, we have calculated the forbidden and radiative corrections to the  $^8\text{Li}$  beta and  $^8\text{B}$  neutrino spectra and have considered the effects of theoretical and experimental uncertainties on the above-mentioned ratio.

In Sec. II we define more carefully the quantities involved and outline the suggested strategy. In Sec. III we give some calculated results, and in Sec. IV we summarize our findings. Most of the formulae have been relegated to appendices.

## II. THE MEASURED QUANTITIES

The recoil electrons produced by  $^8\text{B}$  solar neutrinos being absorbed on deuterium have an average kinetic energy (for an ideal detector) given by

$$\langle T_e \rangle_\nu^{\text{ideal}} = \frac{\int_{T_{\min}} dT_e T_e \int dE_\nu \lambda_\nu(E_\nu) P_{ee}(E_\nu) \frac{d\sigma_{CC}}{dT_e}(E_\nu)}{\int_{T_{\min}} dT_e \int dE_\nu \lambda_\nu(E_\nu) P_{ee}(E_\nu) \frac{d\sigma_{CC}}{dT_e}(E_\nu)}, \quad (1)$$

where  $T_{\min}$  is the threshold kinetic energy below which events in SNO will be discarded. For the discussions that follow, we adopt  $T_{\min} = 5$  MeV. The charge-current differential cross-

section for neutrino absorption on deuterium  $d\sigma_{CC}/dT_e$ , is a function of neutrino energy. We will use the calculated cross-section of Ellis and Bahcall [4] for our computations, and adopt from Bahcall and Lisi [5] a 0.14 %  $1\sigma$  error in  $\langle T_e \rangle_\nu$ , this being the difference when Kubodera-Nozawa cross-sections [6] are used instead. The  ${}^8\text{B}$  neutrino spectrum is denoted  $\lambda_\nu(E_\nu) \equiv d\Gamma/dE_\nu$ , and  $P_{ee}(E_\nu)$  is the probability that an electron-neutrino produced at the core of the sun remains an electron-neutrino by the time it is detected on earth. The different neutrino-oscillation scenarios yield different survival functions,  $P_{ee}(E_\nu)$ . In the Standard Model with no neutrino oscillations,  $P_{ee}(E_\nu) = 1$ .

The decay electrons produced in  ${}^8\text{Li}$  beta decay have an average kinetic energy (for an ideal detector) given by

$$\langle T_e \rangle_e^{\text{ideal}} = \frac{\int_{T_{\min}} dT_e T_e \lambda_e(T_e)}{\int_{T_{\min}} dT_e \lambda_e(T_e)}, \quad (2)$$

where  $\lambda_e(T_e) \equiv d\Gamma/dE_e$  is the electron spectrum. The beta decay of  ${}^8\text{Li}$  is the isospin analogue of the beta decay of  ${}^8\text{B}$ ; both populate the same daughter  ${}^8\text{Be}$  states. The  ${}^8\text{Be}$  excited states are unstable and break up into two alpha particles. As a consequence, the shape of the  ${}^8\text{Li}$   $\beta^-$  spectrum and of the  ${}^8\text{B}$  neutrino spectrum deviate significantly from the standard allowed shape. Measurements [7] of the delayed  $\alpha$  spectra allow one to determine the profile of the intermediate  ${}^8\text{Be}$  state and thus to calculate the deviations in the electron and neutrino spectra. This is discussed at length in Bahcall *et al.* [8], where it is shown there is considerable discrepancy among different experiments related to the absolute energy calibration of the alpha particles. Bahcall *et al.* [8] choose to display this uncertainty as a possible offset  $b$  in the energy of the alpha particles from  ${}^8\text{Be}$  break up:  $E_\alpha \rightarrow E_\alpha + b$ . The value of the offset affects the calculated shape of *both* the beta and neutrino spectra. The effective  $3\sigma$  uncertainty of the offset is estimated to be  $b = \pm 0.104$  MeV [8]; this estimate includes theoretical errors. Bahcall *et al.* [8] have tabulated their recommended  ${}^8\text{B}$  neutrino spectrum together with their  $3\sigma$  errors.

In this work we require both a  ${}^8\text{B}$  neutrino spectrum and a  ${}^8\text{Li}$  electron spectrum from decay to the same final states in  ${}^8\text{Be}^*$ , in order to compare the effects of common-mode uncertainties. Therefore we use R-matrix theory to model the profile of the intermediate  ${}^8\text{Be}$  state, and in particular, the R-matrix fits of Barker [9]. To reproduce the possible offset in the energy of alpha particles, we shift the energy of the dominant resonance,  $E_1 \rightarrow E_1 + b'$ , where the offset  $b'$  is obtained from the requirement that this method gives the same error as the Bahcall *et al.* [8] treatment. The same offset is used consistently for both decay spectra. Details of the R-matrix analysis are given in Appendix A.

There are two further differences between the  ${}^8\text{B}$  neutrino spectrum and the  ${}^8\text{Li}$  electron spectrum originating in (a) recoil (or forbidden) corrections and (b) radiative corrections. Details of these have been relegated to Appendices B and C respectively. However, in Figs. 1 and 2 we show plots of these corrections for the individual spectra and their ratio. Although both corrections are energy-dependent and hence a factor in determining  $\langle T_e \rangle$  their ratio is very much less energy dependent. Thus any error in  $\langle T_e \rangle$  associated with determining these corrections is much reduced in considering the ratio  $\langle T_e \rangle_\nu / \langle T_e \rangle_e$ .

In Fig. 1 we show the recoil correction for the  ${}^8\text{B}$  neutrino spectrum and  ${}^8\text{Li}$  electron spectrum for two cases. The calculation is based on the elementary-particle treatment of beta decay of Holstein [10] and the correction depends principally on two parameters:  $b/c$

and  $d/c$ . Here  $b$ ,  $c$  and  $d$  are the weak-magnetism, Gamow-Teller and induced pseudotensor current form factors respectively. The two cases correspond to the induced pseudotensor current being retained in or removed from the calculation. In both cases the ratio is almost independent of energy, indicating little sensitivity to the presence of induced pseudotensor currents.

In Fig. 2 we show the radiative correction for the  ${}^8\text{B}$  neutrino spectrum and  ${}^8\text{Li}$  electron spectrum again for two cases. In the first case, we assume the internal bremsstrahlung photons are not detected and so the energy of the photon is integrated over in obtaining the radiative correction. In this case there is a large difference in the energy dependence between the radiative corrections for the electron and neutrino spectra. In the second case, we account for the fact that in a calorimetric detector such as SNO, the internal bremsstrahlung photons from a  ${}^8\text{Li}$  source placed in the detector would be recorded and summed with the beta energy. We assume, for simplicity, that the efficiency and detector response for electrons and photons is the same, and compute the radiative correction for the summed energy (photons plus electrons) deposited. Now one sees there is a much reduced difference between the energy dependence of the radiative corrections for the electron and neutrino spectra.

From Figs. 1 and 2, it is fairly clear there will be little uncertainty in the ratio,  $\langle T_e \rangle_\nu / \langle T_e \rangle_e$ , arising from any uncertainty in recoil and radiative corrections. Therefore, we will not consider these corrections explicitly any further; but rather we will assume they are effectively absorbed in the energy offset parameter,  $b$ , which as has been mentioned above was estimated by Bahcall *et al.* [8] to be  $\pm 104$  keV, and contained theoretical uncertainties associated with recoil and radiative corrections.

Finally, we turn to detector-related uncertainties. The measured electron kinetic energy,  $T_e$ , determined by SNO will be distributed around the true energy,  $T'_e$ , with a width established by the detected Cerenkov photon statistics. The resolution function  $R(T'_e, T_e)$  is approximated by a normalized Gaussian:

$$R(T'_e, T_e) = \frac{1}{\sigma(2\pi)^{1/2}} \exp \left\{ -\frac{(T'_e - T_e)^2}{2\sigma^2} \right\}, \quad (3)$$

where  $\sigma \equiv \sigma(T'_e)$  is an energy-dependent  $1\sigma$  width given by [5]

$$\sigma(T'_e) = \sigma_{10} \sqrt{\frac{T'_e}{10 \text{ MeV}}}, \quad (4)$$

with  $\sigma_{10}$  the resolution width at  $T'_e = 10$  MeV. We follow Bahcall and Lisi [5] and use  $\sigma_{10} = 1.1 \pm 0.11$  MeV ( $1\sigma$  errors) as an illustrative example.

The expressions, Eqs. (1) and (2), are now modified to include a response function

$$\langle T_e \rangle_\nu = \frac{\int_{T_{\min}} dT_e T_e \int dE_\nu \lambda_\nu(E_\nu) P_{ee}(E_\nu) \int dT'_e R(T'_e, T_e) \frac{d\sigma_{CC}}{dT'_e}(E_\nu)}{\int_{T_{\min}} dT_e \int dE_\nu \lambda_\nu(E_\nu) P_{ee}(E_\nu) \int dT'_e R(T'_e, T_e) \frac{d\sigma_{CC}}{dT'_e}(E_\nu)}, \quad (5)$$

$$\langle T_e \rangle_e = \frac{\int_{T_{\min}} dT_e T_e \int dT'_e R(T'_e, T_e) \lambda_e(T'_e)}{\int_{T_{\min}} dT_e \int dT'_e R(T'_e, T_e) \lambda_e(T'_e)}. \quad (6)$$

The other major uncertainty concerns the absolute energy calibration for the SNO detector. For this, we assume a 1% error at 10 MeV. This can be easily implemented in the calculations by modifying the energy-resolution function, Eq. (3), with the replacement

$$R(T'_e, T_e) \rightarrow R(T'_e + \delta, T_e), \quad (7)$$

where  $\delta = \pm 100$  keV ( $1\sigma$  error).

The above methods for treating detector-related uncertainties are a rough parametrization of detailed considerations regarding the spatial and directional response to energy deposition in the SNO detector. Other sources of uncertainties which have not been taken into account in this work are (a) the energy dependence of the detector efficiency, (b) the statistical and systematic uncertainties associated with background subtraction and neutral-current event separation, (c) the uncertainties in the  ${}^8\text{Li}$  beta-spectrum (as measured in SNO) due to the source container, and (d) the position dependence of the measured energy. Evaluation of the effects of these uncertainties will have to await detailed Monte-Carlo simulations and actual measurements of detector performance when SNO is operational.

### III. THE ERROR BUDGET

Having listed the source of uncertainties, it remains to quantify their contribution to the error budget for the detection of recoil electrons following neutrino absorption on deuterium alone,  $\langle T_e \rangle_\nu$ , or in concert with a calibration experiment with a  ${}^8\text{Li}$  source in the detector,  $\langle T_e \rangle_\nu / \langle T_e \rangle_e$ . The results are given in Table I. The error budget for the former case has been given by Bahcall and Lisi [5] and we follow their example. The statistical error ( $3\sigma$ ) on 5000 CC events is estimated at 0.98% for  $\langle T_e \rangle_\nu$ . In the calibration experiment there will be considerably more events counted, so the statistical uncertainty in the ratio  $\langle T_e \rangle_\nu / \langle T_e \rangle_e$  will be dominated by the 5000 CC neutrino events: we use the same statistical error. For the neutrino-absorption on deuterium, the uncertainty in the absorption cross-section is common to both  $\langle T_e \rangle_\nu$  and  $\langle T_e \rangle_\nu / \langle T_e \rangle_e$ , so again we use the same error. The uncertainty in the neutrino spectrum from the beta decay of  ${}^8\text{B}$  is characterised by the offset parameter,  $b$ , associated with the absolute energy calibration of the  $\alpha$ -particles in the measured delayed  $\alpha$ -spectrum. Upto differences associated with isospin-symmetry breaking, recoil and radiative corrections, the same uncertainty occurs in the calibration experiment, so the error in the ratio  $\langle T_e \rangle_\nu / \langle T_e \rangle_e$  is much reduced. Table I shows a reduction of uncertainty by a factor of 7.6. The same reasoning follows for the detector-related uncertainties, since in both experiments, energetic electrons are being counted in the same detector. We find a reduction in uncertainty by a factor of 8.5 due to the detector's energy resolution, and a factor of 5.0 due to its absolute energy calibration. The energy calibration of the detector here has been oversimplified. The analysis above assumes that the electron sources from  ${}^8\text{Li}$  beta decay and from neutrino absorption are identical, but of course they are not. The  ${}^8\text{Li}$  calibration sources are highly localized in space and time, while the recoil electrons produced by absorption of solar neutrinos are distributed throughout the detector and distributed in time. So our analysis here represents an optimal scenario, but it is sufficient to make the point that an improvement in the error budget will be achieved by performing an in situ calibration experiment.

If all errors are added together in quadrature, then the  $3\sigma$  uncertainty in the CC test at SNO using  $\langle T_e \rangle_\nu$  alone is 2.8% and is dominated by the uncertainty in the absolute energy calibration. However, in combination with a  $^8\text{Li}$  calibration experiment, the  $3\sigma$  uncertainty in the ratio  $\langle T_e \rangle_\nu / \langle T_e \rangle_e$  is reduced to 1.2%, and more importantly, is dominated by counting statistics. This analysis strategy will significantly improve SNO's ability to discriminate among the different neutrino-oscillation scenarios. In Fig. 3 we display the error budget together with the theoretical value of  $\langle T_e \rangle_\nu / \langle T_e \rangle_e$  for various neutrino-oscillation solutions [11] to the solar-neutrino problem: the two (best-fit) Mikheyev-Smirnov-Wolfenstein (MSW) solutions at small and large mixing angle (SMA and LMA) and the purely vacuum (VAC) oscillation solution. In an analogous plot by Bahcall and Lisi [5], it is shown that a measurement of  $\langle T_e \rangle_\nu$  alone is unlikely to resolve the two MSW solutions. On the other hand, the ratio measurement, Fig. 3, clearly shows the LMA and SMA solutions as being experimentally distinguishable, if the other uncertainties in the detector can be minimized.

Although we have considered the ratio of  $\langle T_e \rangle_\nu / \langle T_e \rangle_e$ , it is possible to construct other experimental quantities from the measured CC and  $^8\text{Li}$  spectra. One of the simplest observables to consider is the actual ratio of the normalized measured CC spectrum,  $\lambda_{exp}^{CC}$ , to the normalized measured  $^8\text{Li}$  electron spectrum,  $\lambda_{exp}^{Li}$ . Because of the high degree of similarity between those two spectra, the effect of uncertainties on the detector response function are expected to largely cancel when forming this ratio. In Fig. 4 we display the effect of the uncertainty in the detector energy scale,  $\delta$  on the the double ratio

$$R(CC/^8Li) = \frac{\lambda_{exp}^{CC} / \lambda_{theor}^{CC}}{\lambda_{exp}^{Li} / \lambda_{theor}^{Li}} \quad (8)$$

where  $\lambda_{theor}$  refers to a spectrum where all parameters including the absolute energy calibration are assumed to be known. If  $\lambda_{exp}^{Li}$  is not measured (i.e. the denominator is assumed to be unity), then the dashed lines enclose the error band with  $\pm 3\sigma$  errors on  $\delta$ . A measurement of  $\lambda_{exp}^{Li}$  allows the cancellation of correlated errors and produces the much reduced “ $\pm 3\sigma$ ” error band enclosed by the solid lines. The effect due to the statistics of 5000 CC events above 5 MeV is shown by overlaying on Fig. 4 the shape distortion expected for the best-fit mass and mixing values for the SMA solution [11] ( $\Delta m^2 = 5.4 \times 10^{-6} \text{ eV}^2$  and  $\sin^2 2\theta = 7.9 \times 10^{-3}$ ). We can clearly see that making use of the  $^8\text{Li}$  spectrum as measured in SNO reduces the effects of systematic uncertainties and greatly increases the discriminating power of the CC shape measurement.

#### IV. SUMMARY

The SNO detector is being constructed primarily to measure the neutral-current (NC) to charged-current (CC) cross-section ratio for solar neutrino absorption in deuterium. It is anticipated this measurement will give a strong and unambiguous signal of neutrino oscillations (or the lack thereof). Another test, which does not rely on the knowledge of the absolute reaction cross-sections, is a measurement of the spectral shape of the CC reaction alone. To improve the sensitivity for this measurement, a calibration experiment is planned at SNO with a  $^8\text{Li}$  source placed in the detector. If instead of considering only the first moment of the recoil electron spectrum in the CC reaction,  $\langle T_e \rangle_\nu$ , the ratio of this moment

to the equivalent moment in the  ${}^8\text{Li}$  beta decay is used as a benchmark, then an increase in the sensitivity of a factor of 2.4 could be achieved in the CC-shape test. This improvement would be sufficient to resolve the small-angle and large-angle MSW solutions to the solar-neutrino problem. We stress again, however, that not all uncertainties are known at the present time and some will require actual measurements when SNO is operational, so our analysis here represents an optimistic best-case scenario. To us, a calibration experiment with a  ${}^8\text{Li}$  source certainly seems beneficial.

## V. ACKNOWLEDGEMENT

We thank Emanuel Bonvin for initially suggesting the use of  ${}^8\text{Li}$  to calibrate the SNO detector, and Graham Lee-Whiting for fruitful discussions on radiative corrections. We also thank J.N. Bahcall and E. Lisi for permission to use their computer code for the calculation of the neutrino-deuterium cross sections.

## APPENDIX A: R-MATRIX FIT

The allowed  $\beta$ -transitions from the decay of  ${}^8\text{Li}$  or  ${}^8\text{B}$  populate  $2^+$  states of  ${}^8\text{Be}$ , which then decay into two  $\alpha$ -particles. The  $\alpha$ -spectra show a pronounced peak, corresponding to the  $2^+$  first excited state of  ${}^8\text{Be}$  at  $E_x \simeq 3.0$  MeV. Attempts to fit the  $\alpha$ -spectra assuming only one state in  ${}^8\text{Be}$  is operative fail to give enough yield at high energies. Barker [12] proposed R-matrix formulae in the many-level, one-channel approximation and used them to fit the  $\beta$ -delayed  $\alpha$ -spectra. More recent fits have been given by Warburton [13] and Barker [9].

In the many-level, one-channel approximation the beta-decay differential cross-section is written

$$d\Gamma \propto \frac{1}{\pi} g(E_x) p_e E_e E_\nu^2 F(\pm Z, E_e) \delta(Q_{ec} + m - E_x - E_e - E_\nu) dE_x dE_e dE_\nu, \quad (\text{A1})$$

where  $Q_{ec} + m = M - M'$ , with  $M$  the mass of the parent nucleus,  $M'$  the ground-state mass of the daughter nucleus and  $m$  the electron mass. Here  $E_x$  is the excitation energy in the daughter nucleus,  $E_e$  the electron energy,  $p_e$  the electron momentum and  $F(Z, E_e)$  the usual Fermi function. This expression differs from the standard one by the presence of the function  $g(E_x)/\pi$  and an additional integration,  $dE_x$ , over the excitation energy of the daughter nucleus.

The function  $g(E_x)$  in R-matrix theory is

$$\begin{aligned} g(E_x) &= \frac{|R_2(E_x)|^2 P_2(E_x)}{|1 - (S_2(E_x) - B_2 + iP_2(E_x)) R(E_x)|^2}, \\ R_2(E_x) &= \sum_\lambda \frac{\gamma_\lambda (M_{GT})_\lambda}{E_\lambda - E}, \\ R(E_x) &= \sum_\lambda \frac{\gamma_\lambda^2}{E_\lambda - E}, \end{aligned} \quad (\text{A2})$$

where  $E$  is the channel energy, *i.e.* the energy above the  $\alpha + \alpha$  threshold:  $E = E_x + 0.092$  MeV. Here  $P_2(E)$  and  $S_2(E)$  are the penetrability and shift factors for  $L = 2$  partial waves and are expressed in terms of Coulomb functions for  $\alpha + \alpha$  scattering evaluated at a chosen channel radius,  $a_2$ . Finally,  $B_2$  is the boundary condition parameter. The sum over  $\lambda$  is a sum over all resonances retained in the calculation. For each resonance there are three parameters:  $E_\lambda$  the centroid energy of the resonance,  $\gamma_\lambda$  the reduced width amplitude for  $\alpha + \alpha$  scattering, and  $(M_{GT})_\lambda$  the Gamow-Teller matrix element for the beta-decay feeding of the resonance.

In the limit of a single narrow resonance,  $\gamma_\lambda^2 P_2 \rightarrow 0$ , then

$$g(E_x) \rightarrow (M_{GT})_\lambda^2 \pi \delta(E_\lambda - E) \quad (\text{A3})$$

and the rate expression, Eq. (A1), reduces to the standard one. To obtain the electron spectrum, we integrate Eq. (A1) over neutrino energies

$$\frac{d\Gamma}{dE_e} \propto p_e E_e F(\pm Z, E_e) \frac{1}{\pi} \int_0^{Q_{ec} + m - E_e} dE_x g(E_x) (Q_{ec} + m - E_x - E_e)^2, \quad (\text{A4})$$

while for the neutrino spectrum, we integrate over electron energies

$$\frac{d\Gamma}{dE_\nu} \propto E_\nu^2 \frac{1}{\pi} \int_0^{Q_{ec} - E_\nu} dE_x g(E_x) \beta(Q_{ec} + m - E_x - E_\nu)^2 F(\pm Z, Q_{ec} + m - E_x - E_\nu), \quad (\text{A5})$$

where  $\beta = p_e/E_e = [1 - m^2/(Q_{ec} + m - E_x - E_\nu)^2]^{1/2}$ .

It remains to specify the parameters, which we take from the work of Barker [9], where fits are made simultaneously to the  $\alpha + \alpha$  scattering  $d$ -wave phase shift as well as the beta-delayed  $\alpha$ -spectra. Separate fits, however, are done for the  ${}^8\text{B}$  and  ${}^8\text{Li}$  beta-delayed  $\alpha$ -spectra. Thus there are differences in the parameter sets between the two cases. However, these differences are small and can be attributable to isospin-symmetry breaking. The adjustable parameters in the formulae include the channel radius  $a_2$ , the boundary condition parameter  $B_2$ , and the eigenenergies  $E_\lambda$ , reduced width amplitudes  $\gamma_\lambda$  and Gamow-Teller matrix elements  $(M_{GT})_\lambda$  for the various  $2^+$  levels,  $\lambda$ . The best fits were obtained with a large channel radius of  $a_2 \simeq 6.5$  fm. For this value of  $a_2$ , the second  $2^+$  level is at about 9 MeV, with a width of about 10 MeV. To date, there is no evidence for a state in this vicinity. Altogether five resonances are included, denoted  $\lambda = 1, 2, 3, 0, 1'$ . The state,  $\lambda = 1$ , is the dominant resonance corresponding to the first excited state in  ${}^8\text{Be}$  at about 3 MeV; while  $\lambda = 2$  is the second  $2^+$  state just mentioned, and  $\lambda = 3$  represents a background state well above the energy range being fitted and which naturally is not fed in beta decay,  $(M_{GT})_3 = 0$ . In addition, there are two narrow states at  $E_x = 16.6$  and 16.9 MeV, which are isospin mixtures of  $T = 0$  and  $T = 1$   $2^+$  states, the latter being the analogue of the ground states of  ${}^8\text{Li}$  and  ${}^8\text{B}$  and is fed by Fermi beta decay,  $(M_F)_{1'} = \sqrt{2}$ . The method of handling this isospin mixing is described in Barker [12] and Warburton [13].

The fitted parameters  $E_\lambda$ ,  $\gamma_\lambda$  and  $(M_{GT})_\lambda$  depend on the choice  $B_2$ . Identical fits can be found for different choices; and connection formulae are available [14] to relate one set of fitted parameters to another. The standard choice is to set  $B_2 = S_2(E_\mu)$ , where  $\mu$  is one of the resonances of the fit. The parameters obtained with this choice are labelled  $E_\lambda^{(\mu)}$ ,  $\gamma_\lambda^{(\mu)}$  and  $(M_{GT})_\lambda^{(\mu)}$ . Barker [9] only gives the parameter values for the case  $\mu = \lambda$ , and the connection



formulae have to be used to relate them all to a common  $B_2$  value. This is cumbersome to use; for our purposes it is sufficiently accurate to take the parameter values for  $\mu = \lambda$  and to vary  $B_2$  as follows: for  $E_x < 5$  MeV where the  $\lambda = 1$  resonance dominates, use  $B_2 = S_2(E_1)$ ; for  $5 < E_x < 13$  MeV where the  $\lambda = 2$  resonance dominates, use  $B_2 = S_2(E_2)$ ; and for  $E_x > 13$  MeV where the doublet states dominate, use  $B_2 = S_2(\overline{E})$ , where  $\overline{E}$  is the average energy of the two isospin-mixed states. The parameter values are given in Table II.

## APPENDIX B: RECOIL CORRECTIONS

Recoil corrections to allowed beta decay have been given by Holstein [10] and used by Bahcall and Holstein [15] in their discussion of corrections to the spectrum of neutrinos produced by the beta decay of  $^8\text{B}$  in the sun. There are two sources to the recoil corrections: (a) true kinematic corrections arising from relaxing the approximation that the recoiling nucleus is at rest, and (b) the introduction of induced terms into the V-A weak hadronic current, mainly the induced tensor term in the vector current (weak magnetism) and the induced pseudotensor term in the axial current. We have not included an induced scalar term in the vector current, as it gives a zero contribution under the assumption of the conserved vector current (CVC) hypothesis, or an induced pseudoscalar term in the axial current as it is small in beta decay. The beta decay spectrum, therefore, is predominantly given by four form factors, denoted in the formalism of Holstein [10] by  $a$ ,  $b$ ,  $c$  and  $d$  for the Fermi, weak magnetism, Gamow-Teller and induced pseudotensor current form factors respectively.

Let  $P$ ,  $p_r$ ,  $p_e$  and  $p_\nu$  denote the respective four momenta of the parent nucleus, daughter nucleus, electron and neutrino. Further, let  $M$  be the mass of the parent nucleus,  $M_N(^8\text{Li})$  or  $M_N(^8\text{B})$ ;  $M'$  be the ground-state mass of the daughter nucleus,  $M_N(^8\text{Be})$ ;  $E_x$  the excitation energy above the ground state; and  $m$  the mass of the electron<sup>1</sup>. Then we define

$$\begin{aligned} q &= P - p_r = p_e + p_\nu, \\ \Delta &= M - M' - E_x. \end{aligned} \tag{B1}$$

Further the maximum electron energy is

$$\begin{aligned} A_0 &= (M^2 + m^2 - M'^2)/2M \\ &\simeq \Delta - \frac{\Delta^2 - m^2}{2M}, \end{aligned} \tag{B2}$$

and the maximum neutrino energy is

$$\begin{aligned} C_0 &= [M^2 - (m + M')^2]/2M, \\ C_0 + m &\simeq \Delta - \frac{(\Delta - m)^2}{2M}. \end{aligned} \tag{B3}$$

---

<sup>1</sup>Holstein [10] writes  $M_1$  and  $M_2$  as the masses of the parent and daughter nuclei respectively, and  $M$  as their arithmetic mean.

The form factors are functions of the four-momentum transfer squared. It is convenient to expand these form factors

$$\begin{aligned}
a(q^2) &= a_1 + a_2(q^2/M^2) + \dots, \\
c(q^2) &= c_1 + c_2(q^2/M^2) + \dots, \\
b(q^2) &= b + \dots, \\
d(q^2) &= d + \dots
\end{aligned} \tag{B4}$$

and retain just the terms shown. In the formulae that follow, we will drop the dependence on the four-momentum transfer, *i.e.* neglect  $a_2$  and  $c_2$ , and not display the electromagnetic corrections, which are of order  $(\alpha Z)$ . Both these effects are very small on the recoil corrections, although they are retained in the final computations.

The probability that an electron of energy,  $E_e$ , is produced in an allowed transition in beta decay is proportional to

$$\frac{d\Gamma}{dE_e} \propto (a_1^2 + c_1^2) F(\pm Z, E_e) (\Delta - E_e)^2 p_e E_e r_e(E_e), \tag{B5}$$

where  $r_e(E_e)$  is the recoil correction,  $F(\pm Z, E_e)$  is the usual Fermi function and  $p_e$  is the electron momentum,  $p_e = [E_e^2 - m^2]^{1/2}$ . The upper sign is for electron emission in  $\beta^-$  decay, the lower sign for positron emission in  $\beta^+$  decay. The recoil correction is

$$\begin{aligned}
r_e(E_e) &= \left\{ 1 - \frac{2}{3} \frac{\Delta}{M} \frac{(c_1^2 + c_1 d \pm c_1 b)}{(a_1^2 + c_1^2)} + \frac{2}{3} \frac{E_e}{M} \frac{(3a_1^2 + 5c_1^2 \pm 2c_1 b)}{(a_1^2 + c_1^2)} \right. \\
&\quad \left. - \frac{1}{3} \frac{m^2}{M E_e} \frac{(2c_1^2 + c_1 d \pm 2c_1 b)}{(a_1^2 + c_1^2)} \right\} \frac{(A_0 - E_e)^2}{(\Delta - E_e)^2}.
\end{aligned} \tag{B6}$$

This result has been given before by Holstein [10].

For the neutrino spectrum, the probability that a neutrino of energy,  $E_\nu$ , is produced in an allowed transition in beta decay is proportional to

$$\frac{d\Gamma}{dE_\nu} \propto (a_1^2 + c_1^2) F(\pm Z, \Delta - E_\nu) E_\nu^2 (\Delta - E_\nu) [(\Delta - E_\nu)^2 - m^2]^{1/2} r_\nu(E_\nu), \tag{B7}$$

where  $r_\nu(E_\nu)$  is the recoil correction given by

$$\begin{aligned}
r_\nu(E_\nu) &= \left\{ 1 - \frac{m\Delta}{M} \left[ \frac{1}{\Delta - E_\nu} + \frac{1}{\Delta - E_\nu + m} \right] \right. \\
&\quad \left. - \frac{2}{3} \frac{\Delta}{M} \frac{(c_1^2 + c_1 d \mp c_1 b)}{(a_1^2 + c_1^2)} + \frac{2}{3} \frac{E_\nu}{M} \frac{(3a_1^2 + 5c_1^2 \mp 2c_1 b)}{(a_1^2 + c_1^2)} \right. \\
&\quad \left. + \frac{1}{3} \frac{m^2}{M(\Delta - E_\nu)} \frac{(2c_1^2 - c_1 d \mp 2c_1 b)}{(a_1^2 + c_1^2)} \right\} \frac{(C_0 + m - E_\nu) [(C_0 + m - E_\nu)^2 - m^2]^{1/2}}{(\Delta - E_\nu) [(\Delta - E_\nu)^2 - m^2]^{1/2}}.
\end{aligned} \tag{B8}$$

Note that  $r_\nu(E_\nu)$  is not given by  $r_e(E_e \rightarrow \Delta - E_\nu)$ . The reason is that, in recoil order, the energy available is distributed three ways: to the electron, to the neutrino and to the

recoiling nucleus. The replacement  $E_e \rightarrow \Delta - E_\nu$  is only correct in the approximation that the recoiling nucleus is at rest.

It remains to specify the values for the form factors. For the dominant transition in the decay of  ${}^8\text{B}$  or  ${}^8\text{Li}$ ,  $2^+, T = 1 \rightarrow 2^+, T = 0$ , the transition is pure Gamow-Teller and  $a_1 = 0$ . Then, for the recoil correction it is only necessary to supply the ratios  $b/c_1$  and  $d/c_1$ . For these we use the same values as Bahcall and Holstein [15]:

$$\begin{aligned}\frac{b}{Ac_1} &= 7.7 \pm 1.0, \\ \frac{d}{Ac_1} &= 1.9 \pm 1.3,\end{aligned}\tag{B9}$$

where  $A$  is the mass number,  $A = 8$ . The weak magnetism value is determined from the CVC hypothesis and the measurement of the M1 width of the  $2^+$  analogue state in  ${}^8\text{Be}$  [16]. This value is consistent with, but less precise than, the recent measurement of the M1 width of de Braeckeler *et al.* [17]. The induced pseudotensor form-factor value is determined from fits to the measured  $\beta$ - $\alpha$  correlations on  ${}^8\text{B}$  and  ${}^8\text{Li}$  [18]. The form factor  $d$  is the lesser precisely known of the two listed in Eq. (B9). To sample the dependence on  $d$ , some results will be given for  $d = 0$ .

### APPENDIX C: RADIATIVE CORRECTIONS

Radiative corrections to the electron spectrum from allowed beta decay have been considered in a number of papers [19–23]. In obtaining the corrections, integrations are carried out over the allowed neutrino and photon energies and the results exhibited as a differential spectrum in electron energy. The contributions to the radiative corrections have two components: the emission of real photons (internal bremsstrahlung) and virtual radiative corrections due, for example, to the exchange of photons between charged particles. The differential rate for real photon emission in an allowed beta transition is given by the expression [24]

$$\begin{aligned}d\Gamma &\propto \frac{\alpha}{2\pi} \frac{1}{\epsilon} Q^2 dQ E_\nu^2 dE_\nu p_e E_e dE_e dx \delta(\Delta - E_e - E_\nu - \epsilon) \\ &\times \left[ \left( \frac{E_e + \epsilon}{E_e} \right) \frac{\beta^2(1 - x^2 Q^2/\epsilon^2)}{(\epsilon - \beta Qx)^2} + \frac{\epsilon}{E_e^2(\epsilon - \beta Qx)} \right].\end{aligned}\tag{C1}$$

Here  $\epsilon$  represents the photon energy,  $\epsilon = [Q^2 + \lambda^2]^{1/2}$ ,  $Q$  being the photon momentum and  $\lambda$  a small nonzero photon mass introduced to regulate the infrared divergence. Further,  $E_e$  is the electron energy,  $p_e$  the electron momentum,  $\beta = p_e/E_e$ ,  $\Delta$  the maximum electron energy and  $x$  the cosine of the angle between the electron and photon directions. The delta function is used to integrate over the neutrino energies. The integrations over  $Q$  and  $x$  are however very delicate: the logarithmic pole in  $\lambda$  has to be extracted to cancel with the  $\lambda$  dependence coming from the virtual corrections.

In the calibration experiment at SNO, a  ${}^8\text{Li}$  source will be placed inside the SNO detector. The real internal bremsstrahlung photons emitted by this source will in principle be detected. So we cannot follow the normal procedure of obtaining the radiative correction by integrating

over  $Q$ . Suppose that SNO detects photons of energy greater than some threshold, say  $\omega$ . Then for  $Q$  less than  $\omega$ , the normal procedure can be followed except that in the integration over  $Q$ , the upper limit  $Q_{\max}$  is taken to be the lesser of  $\omega$  or  $\Delta - E_e$ , rather than just  $\Delta - E_e$ . The result for real photon emission is

$$\begin{aligned} \frac{d\Gamma}{dE_e} &\propto (\Delta - E_e)^2 p_e E_e \frac{\alpha}{\pi} g_{<}(E_e, \Delta) \\ g_{<}(E_e, \Delta) &= \frac{1}{E_e^2 y^2} \left[ \frac{1}{2} y^2 Q_{\max}^2 - \frac{2}{3} y Q_{\max}^3 + \frac{1}{4} Q_{\max}^4 \right] \frac{1}{2\beta} \ln \left( \frac{1+\beta}{1-\beta} \right) \\ &\quad + \frac{2}{y^2 E_e} \left[ (y^2 - 2yE_e) Q_{\max} + \frac{1}{2} (E_e - 2y) Q_{\max}^2 + \frac{1}{3} Q_{\max}^3 \right] \left[ \frac{1}{2\beta} \ln \left( \frac{1+\beta}{1-\beta} \right) - 1 \right] \\ &\quad + 2 \ln \left( \frac{Q_{\max}}{\lambda} \right) \left[ \frac{1}{2\beta} \ln \left( \frac{1+\beta}{1-\beta} \right) - 1 \right] + \mathcal{C}, \end{aligned} \quad (\text{C2})$$

where  $y$  is  $(\Delta - E_e)$ , and  $Q_{\max}$  the lesser of  $\omega$  or  $y$ . The value of  $\mathcal{C}$  is given by Kinoshita and Sirlin [19]

$$\begin{aligned} \mathcal{C} &= 2 \ln 2 \left[ \frac{1}{2\beta} \ln \left( \frac{1+\beta}{1-\beta} \right) - 1 \right] + 1 + \frac{1}{4\beta} \ln \left( \frac{1+\beta}{1-\beta} \right) \left[ 2 + \ln \left( \frac{1-\beta^2}{4} \right) \right] \\ &\quad + \frac{1}{\beta} [L(\beta) - L(-\beta)] + \frac{1}{2\beta} \left[ L \left( \frac{1-\beta}{2} \right) - L \left( \frac{1+\beta}{2} \right) \right], \end{aligned} \quad (\text{C3})$$

where  $L(z)$  is a Spence function

$$L(z) = \int_0^z \frac{dt}{t} \ln(|1-t|). \quad (\text{C4})$$

For the case when the photon energy exceeds  $\omega$  we must proceed a little differently. We assume, for simplicity, that photons and electrons are detected with equal efficiency and that it is the sum of the energy deposited that is observed in the SNO detector. Thus in Eq. (C1) we change variables from  $dE_e dQ$  to  $dE_e dX$ , where  $X$  is the sum  $E_e + Q$ , and integrate over  $E_e$  from  $m$  to  $X$ . The result is

$$\begin{aligned} \frac{d\Gamma}{dX} &\propto (\Delta - X)^2 \beta(X) X^2 \frac{\alpha}{\pi} g_{>}(X, \Delta), \\ g_{>}(X, \Delta) &= \frac{2}{\beta(X)X} F(X) \ln \left( \frac{X-m}{\lambda} \right) - \frac{2}{\beta(X)X} \int_m^X dE \frac{F(X) - F(E)}{X-E} \\ &\quad + \frac{1}{2} \frac{(XJ_1 - J_2)}{\beta(X)X^2}, \end{aligned} \quad (\text{C5})$$

where

$$\begin{aligned} J_1 &= \int_m^X dE \ln \left( \frac{1+\beta}{1-\beta} \right), \\ J_2 &= \int_m^X dE E \ln \left( \frac{1+\beta}{1-\beta} \right), \\ F(E) &= \beta E \left[ \frac{1}{2\beta} \ln \left( \frac{1+\beta}{1-\beta} \right) - 1 \right] \end{aligned} \quad (\text{C6})$$

and  $\beta \equiv \beta(E) = (1 - m^2/E^2)^{1/2}$ . To these expressions must be added the contribution from virtual radiative corrections, which have been given by Yokoo *et al.* [22]. The result is

$$\begin{aligned} \frac{d\Gamma}{dE_e} &\propto (\Delta - E_e)^2 p_e E_e \frac{\alpha}{\pi} g_v(E_e, \Delta), \\ g_v(E_e, \Delta) &= \mathcal{A} + 3 \ln\left(\frac{\Lambda}{M}\right) + \frac{3}{4}, \\ \mathcal{A} &= \frac{1}{2}\beta \ln\left(\frac{1+\beta}{1-\beta}\right) - 1 + 2 \ln\left(\frac{\lambda}{m}\right) \left[ \frac{1}{2\beta} \ln\left(\frac{1+\beta}{1-\beta}\right) - 1 \right], \\ &\quad + \frac{3}{2} \ln\left(\frac{M}{m}\right) - \frac{1}{\beta} \left[ \frac{1}{2} \ln\left(\frac{1+\beta}{1-\beta}\right) \right]^2 + \frac{1}{\beta} L\left(\frac{2\beta}{1+\beta}\right) \end{aligned} \quad (\text{C7})$$

where  $M$  is the nucleon mass, and  $\Lambda$  a renormalization scale. In the early years, Yokoo *et al.* [22] invoked an intermediate vector-boson model to argue that  $\Lambda$  should be of the order of the nucleon mass. Following the development of the Weinberg-Salam Standard Model, the virtual radiative correction includes additionally the exchange of  $Z$ -bosons. Sirlin [21] has shown, remarkably, that the form of the expression, Eq. (C7), remains unchanged except that  $\Lambda$  is now replaced by the mass of the  $Z$ -boson,  $m_Z$ . For our purposes, the value of  $\Lambda$  is not important as it only enters in a constant, energy-independent term and would be absorbed into the normalization of the spectra. In Fig. 2 we used  $\Lambda$  equal to the nucleon mass,  $M$ . Note that the infrared divergence term in  $\ln(\lambda)$  exactly cancels between the real and virtual photon expressions, as it should. In summary, the radiative correction to the electron spectrum is

$$\begin{aligned} \frac{d\Gamma}{dE} &\propto (\Delta - E)^2 \beta(E) E^2 R_e(E, \Delta), \\ R_e(E, \Delta) &= 1 + \frac{\alpha}{\pi} (g_<(E, \Delta) + g_v(E, \Delta)) \quad \text{for } E = E_e < \omega, \\ &= 1 + \frac{\alpha}{\pi} (g_>(E, \Delta) + g_v(E, \Delta)) \quad \text{for } E = X \geq \omega. \end{aligned} \quad (\text{C8})$$

Finally, we consider the radiative correction for the neutrino spectrum. This is not obtained from the electron spectrum radiative correction by the substitution of  $E_e \rightarrow \Delta - E_\nu$  because the energy available to the leptons is distributed three ways: to the electron, to the neutrino and to the internal bremsstrahlung photon. This was first pointed out by Batkin and Sundaresan [24]. Since the neutrinos are originating from beta decays in the sun, there is no question this time of the internal bremsstrahlung photons being detected. Thus, starting from Eq. (C1) for the real photon radiative correction, the delta function is used in the integration over electron energies, while the integrations over  $Q$  and  $x$  are done carefully to isolate the infrared singularity. The result has been given by Batkin and Sundaresan [24]. The virtual radiative correction is unchanged and given by Eq. (C7). Putting these together we get

$$\begin{aligned} \frac{d\Gamma}{dE_\nu} &\propto E_\nu^2 (\Delta - E_\nu)^2 \beta R_\nu(E_\nu, \Delta), \\ R_\nu(E_\nu, \Delta) &= 1 + \frac{\alpha}{\pi} (g_\nu(E_\nu, \Delta) + g_v(\Delta - E_\nu, \Delta)), \\ g_\nu(E_\nu, \Delta) &= 2 \ln\left(\frac{\Delta - E_\nu - m}{\lambda}\right) \left[ \frac{1}{2\beta} \ln\left(\frac{1+\beta}{1-\beta}\right) - 1 \right] + \mathcal{C} + \frac{1}{2(\Delta - E_\nu)^2 \beta} I_1 + I_2, \end{aligned} \quad (\text{C9})$$

where

$$\begin{aligned}
I_1 &= \int_0^{\Delta - E_\nu - m} dQ Q \ln \left( \frac{1 + \beta(Q)}{1 - \beta(Q)} \right), \\
I_2 &= \int_0^{\Delta - E_\nu - m} dQ \frac{Q}{2\beta(\Delta - E_\nu)} \left[ [(\Delta - E_\nu - Q)^2 - m^2]^{1/2} F(\beta(Q)) \right. \\
&\quad \left. - [(\Delta - E_\nu)^2 - m^2]^{1/2} F(\beta(0)) \right], \\
F(\beta(Q)) &= \frac{4}{Q^2} \left[ \frac{1}{2\beta(Q)} \ln \left( \frac{1 + \beta(Q)}{1 - \beta(Q)} \right) - 1 \right], \\
\beta(Q) &= \left[ 1 - \frac{m^2}{(\Delta - E_\nu - Q)^2} \right]^{1/2}
\end{aligned} \tag{C10}$$

and  $\beta \equiv \beta(0)$ .

## REFERENCES

- [1] SNO Collaboration, G.T. Ewan *et al.*, “Sudbury Neutrino Observatory Proposal,” Report No. SNO-87-12, 1987 (unpublished)
- [2] J.N. Bahcall, *Neutrino Astrophysics* (Cambridge University Press, Cambridge, England, 1989)
- [3] B. Sur *et al.*, Bull. Am. Phys. Soc. **39**, 1389 (1994)
- [4] S.D. Ellis and J.N. Bahcall, Nucl. Phys. **A114**, 636 (1968)
- [5] J.N. Bahcall and E. Lisi, Phys. Rev. **D54**, 5417 (1996)
- [6] K. Kubodera and S. Nozawa, Int. J. Mod. Phys. **E3**, 101 (1994)
- [7] D.H. Wilkinson and D.E. Alburger, Phys. Rev. Lett. **26**, 1127 (1971); B.J. Farmer and C.M. Class, Nucl. Phys. **15**, 626 (1960); L. De Braekeleer and D. Wright, unpublished data, as quoted in L. De Braekeleer *et al.*, Phys. Rev. **C51**, 1767 (1995)
- [8] J.N. Bahcall, E. Lisi, D.E. Alburger, L. De Braekeleer, S.J. Freedman, and J. Napolitano, Phys. Rev. **C54**, 411 (1996)
- [9] F.C. Barker, Aust. J. Phys., **42**, 25 (1989)
- [10] B.R. Holstein, Rev. Mod. Phys., **46**, 789 (1974)
- [11] J.N. Bahcall and P.I. Krastev, Phys. Rev. **D53**, 4211 (1996)
- [12] F.C. Barker, Aust. J. Phys., **22**, 418 (1969)
- [13] E.K. Warburton, Phys. Rev. **C33**, 303 (1986)
- [14] F.C. Barker, Aust. J. Phys., **25**, 341 (1972)
- [15] J.N. Bahcall and B.R. Holstein, Phys. Rev. **C33**, 2121 (1986)
- [16] A.M. Nathan *et al.*, Phys. Rev. Lett. **35**, 1137 (1975); **49**, 1056(E) (1982)
- [17] L. De Braekeleer *et al.*, Phys. Rev. **C51**, 2778 (1995)
- [18] R.E. Tribble and G.T. Garvey, Phys. Rev. **C12**, 967 (1975); R.D. McKeown *et al.*, Phys. Rev. **C22**, 738 (1980)
- [19] T. Konoshita and A. Sirlin, Phys. Rev. **113**, 1652 (1959)
- [20] A. Sirlin, Phys. Rev. **164**, 1767 (1967)
- [21] A. Sirlin, Rev. Mod. Phys., **50**, 573 (1978)
- [22] Y. Yokoo, S. Suzuki and M. Morita, Prog. Theor. Phys. **50**, 1894 (1973)
- [23] Y. Yokoo and M. Morita, Suppl. Prog. Theor. Phys. **60**, 37 (1976)
- [24] I.S. Batkin and M.K. Sundaresan, Phys. Rev. **D52**, 5362 (1995)

## TABLES

TABLE I. Percentage  $3\sigma$  error in  $\langle T_e \rangle_\nu$  from Bahcall and Lisi [5] and in the ratio,  $\langle T_e \rangle_\nu / \langle T_e \rangle_e$ .

% Error in:	$\langle T_e \rangle_\nu$	$\langle T_e \rangle_\nu / \langle T_e \rangle_e$
Statistics of 5000 CC events	0.98	0.98
CC cross-section	0.43	0.43
Neutrino spectrum	1.14	0.15
Energy resolution	0.94	0.11
Absolute energy calibration	2.04	0.41
Total error	2.82	1.16 <sup>a</sup>

<sup>a</sup>We stress this is an optimistic estimate, see text. When explicit calibration measurements are completed this number could change.

TABLE II. Parameters in the R-matrix fit of Barker [9] to the beta-delayed  $\alpha$ -spectra.

$\lambda$	<sup>8</sup> B decay			<sup>8</sup> Li decay		
	$E_\lambda$ <sup>a</sup>	$\gamma_\lambda$ <sup>b</sup>	$(M_{GT})_\lambda$	$E_\lambda$ <sup>a</sup>	$\gamma_\lambda$ <sup>b</sup>	$(M_{GT})_\lambda$
1	2.804	0.588	0.102	2.798	0.591	0.108
2	8.87	0.884	−0.180	8.85	0.880	−0.181
3	34.1	1.442	0.000	34.1	1.442	0.000
0	16.72	0.109	1.64	16.72	0.109	1.77
1'	17.02	<sup>c</sup>	0.000 <sup>d</sup>	17.02	<sup>c</sup>	0.000 <sup>d</sup>

<sup>a</sup>This is the channel energy in MeV.

<sup>b</sup>In units of MeV<sup>1/2</sup>.

<sup>c</sup> $\alpha$ -decay from  $T = 1$  states is isospin forbidden. However, two-state isospin mixing is included, see text.

<sup>d</sup>However, a Fermi matrix element of  $(M_F)_{1'} = \sqrt{2}$  is included.



## FIGURES

FIG. 1. Recoil corrections, Eqs. (B6) and (B8), for the electron spectrum of  ${}^8\text{Li}$  and the neutrino spectrum of  ${}^8\text{B}$  respectively, and their ratio. Graph (a) includes the induced pseudotensor current form factor; graph(b) excludes the induced pseudotensor current form factor.

FIG. 2. Radiative corrections, Eqs. (C8) and (C9), for the electron spectrum of  ${}^8\text{Li}$  and the neutrino spectrum of  ${}^8\text{B}$  beta decay respectively and their ratio. Graph (a) is the case when the internal bremsstrahlung photons are not detected,  $\omega$  large (see Appendix C); graph (b) is the case when the internal bremsstrahlung photons are detected and the total energy deposited,  $X = E_e + Q$ , is recorded in the SNO detector,  $\omega$  small.

FIG. 3. Values of the ratio,  $\langle T_e \rangle_\nu / \langle T_e \rangle_e$ , and their  $3\sigma$  errors due to various uncertainties. Also shown are various theoretical values corresponding to different neutrino-oscillation scenarios, taken from Bahcall and Lisi [5]. Labels: STD = standard (no oscillation); SMA = small-mixing angle (MSW); LMA = large-mixing angle (MSW); VAC = vacuum oscillation.

FIG. 4. Ratios of normalized electron spectra as a function of the electron kinetic energy,  $T_e$  (see text). The two dashed lines enclose the error band without a  ${}^8\text{Li}$  calibration experiment, due to the  $\pm 3\sigma$  uncertainty in absolute energy calibration. The two solid lines enclose the error band in the ratio of measured  ${}^8\text{B}$  solar-neutrino to measured  ${}^8\text{Li}$  spectra under the same assumptions. The data points are theoretical values for the CC spectrum evaluated under the small-angle MSW solution (SMA).

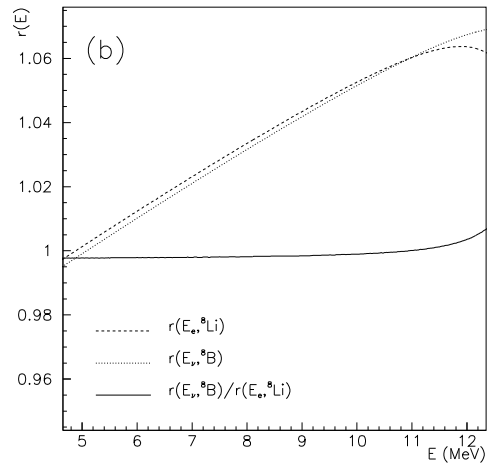
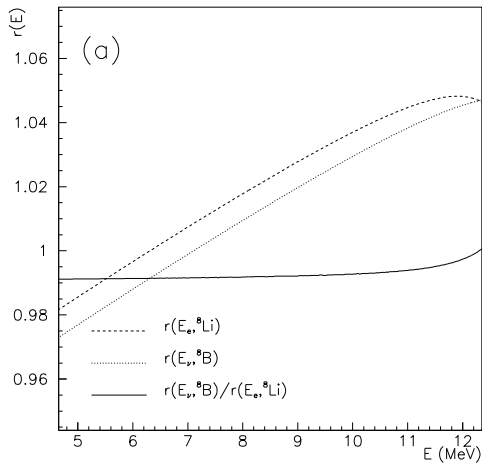


FIG. 1.

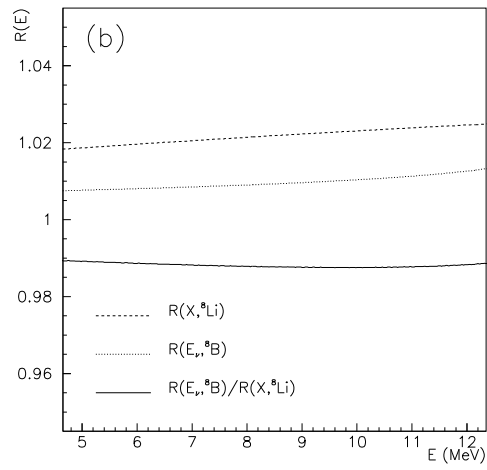
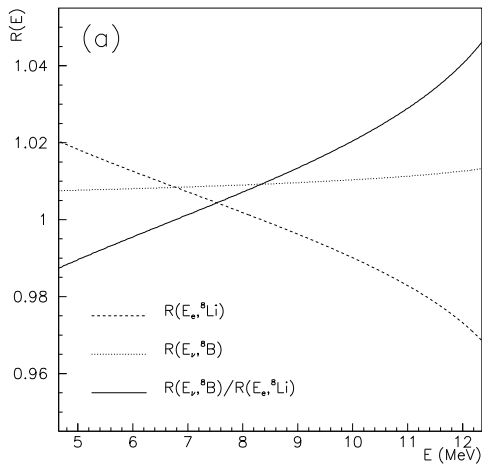


FIG. 2.

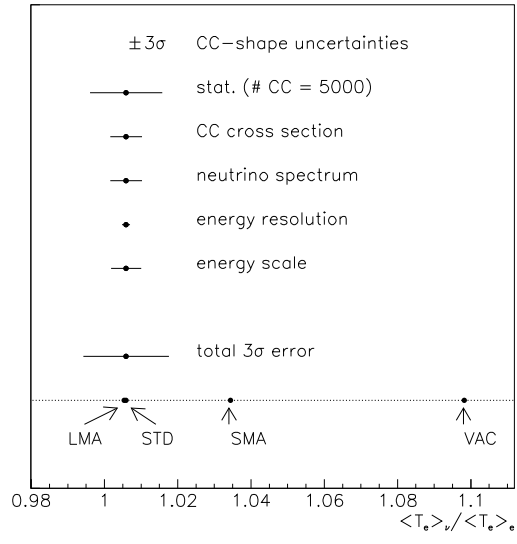


FIG. 3.

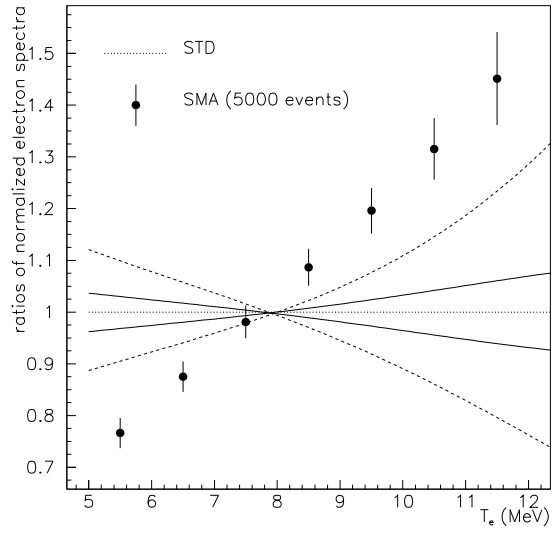


FIG. 4.